The FEBS Journal

FEBS PRESS science publishing by scientists

REVIEW ARTICLE

Ice-binding proteins and the 'domain of unknown function' 3494 family

Tyler D. R. Vance[1], Maddalena Bayer-Giraldi[2], Peter L. Davies[1] and Marco Mangiagalli[3]

1 Department of Biomedical and Molecular Sciences, Queen's University, Kingston, Canada
2 Department of Glaciology, Alfred Wegener Institute Helmholtz Centre for Polar and Marine Research, Bremerhaven, Germany
3 Department of Biotechnology and Biosciences, University of Milano-Bicocca, Italy

Keywords
DUF 3494; IBP-1 fold; ice recrystallization inhibition; ice-binding protein; thermal hysteresis

Correspondence
M. Mangiagalli, Department of Biotechnology and Biosciences, University of Milano-Bicocca, Piazza della Scienza 2, 20126 Milan, Italy
Tel: +39 02 6448 3523
E-mail: m.mangiagalli@campus.unimib.it

(Received 21 November 2018, revised 3 January 2019, accepted 22 January 2019)

doi:10.1111/febs.14764

Ice-binding proteins (IBPs) control the growth and shape of ice crystals to cope with subzero temperatures in psychrophilic and freeze-tolerant organisms. Recently, numerous proteins containing the domain of unknown function (DUF) 3494 were found to bind ice crystals and, hence, are classified as IBPs. DUF3494 IBPs constitute today the most widespread of the known IBP families. They can be found in different organisms including bacteria, yeasts and microalgae, supporting the hypothesis of horizontal transfer of its gene. Although the 3D structure is always a discontinuous β-solenoid with a triangular cross-section and an adjacent alpha-helix, DUF3494 IBPs present very diverse activities in terms of the magnitude of their thermal hysteresis and inhibition of ice recrystallization. The proteins are secreted into the environments around the host cells or are anchored on their cell membranes. This review covers several aspects of this new class of IBPs, which promise to leave their mark on several research fields including structural biology, protein biochemistry and cryobiology.

Introduction

Wide expanses of the Earth experience temperatures seasonally or permanently below zero degrees [1–3]. These regions include sea and lake ice, glaciers, polar ice caps and snow-covered mountains. Subzero temperatures lead to the formation of ice crystals, which can cause cell lysis through changes in osmotic pressure or physical rupture [4,5]. Organisms that face this threat have developed several strategies to combat freezing. One approach is to produce high concentrations of solutes – such as polyalcohols and sugars – to depress the freezing point of water in a colligative manner [6]. Another strategy is to develop ice-binding proteins (IBPs) that adsorb to ice crystals and control their growth in a non-colligative way [7–10].

Ice-binding proteins were first discovered in fishes in the late 1960s and described as antifreeze proteins (AFPs) because they functioned to depress the freezing point of biological fluids [11]. Since then, IBPs performing a variety of biological roles have been isolated and characterized from many different organisms, including fishes, insects, plants, bacteria, fungi and algae [7,12–14]. In higher eukaryotes, two IBP functions that counteract freezing damage are freeze avoidance and freeze tolerance. Freeze-avoiding organisms,

Abbreviations
AFP, antifreeze protein; *Col*IBP, *Colwellia* sp. strain SLW05 ice-binding protein; DUF, domain of unknown function; *Efc*IBP, *Euplotes focardii* bacterial consortium ice-binding protein; *Fc*IBP11, *Fragilariopsis cylindrus* ice-binding protein isoform 11; *Ff*IBP, *Flavobacterium frigoris* PS1 ice-binding protein; FIPA, fluorescence-based ice plane affinity; IBP, ice-binding protein; IBPv, *Flavobacteriaceae* bacterium 3519-10 ice-binding protein; IBS, ice-binding site; IRI, ice recrystallization inhibition; *Le*IBP, *Leucosporidium* sp. AY30 ice-binding protein; *Mp*IBP, *Marinomonas* primoryensis ice-binding protein; *Sf*IBP_1, *Shewanella* frigidimarina ice-binding protein; TH, thermal hysteresis; *Tis*IBP6, *Typhula* ishikariensis ice-binding protein isoform 6; *Tis*IBP8, *Typhula* ishikariensis ice-binding protein isoform 8; Tm, midpoint temperature.

like fishes and insects, produce IBPs to prevent ice crystal growth, thereby maintaining their biological fluids in a liquid state [12,15]. However, IBPs in freeze-tolerant organisms, like plants, function to minimize the damage caused by freezing [16,17]. These latter IBPs are active in inhibiting the growth of harmful large crystals at the expense of smaller ones in the area surrounding the plant cells, a process known as ice recrystallization inhibition (IRI) [16].

The role of IBPs in microorganisms may be more varied. For instance, the Antarctic bacterium *Marinomonas primoryensis* uses a multidomain protein with ice-binding activity to adhere to both diatoms and surface sea-ice, hence forming an oxygen/nutrient-rich zone in their environment [18,19]. Lastly, many different microorganisms isolated from snow, sea-ice and polar terrestrial and marine environments secrete IBPs that, in addition to a freeze tolerance function, potentially increase their habitable space by altering the morphology of surrounding ice [20–25].

Activity-based classification of IBPs

Ice-binding proteins are able to depress the freezing point of water by adsorbing to the surface of nascent ice crystals [26]. Surface adsorption also slightly increases the ice melting temperature [27,28]. This thermal hysteresis (TH), the difference between the melting and freezing points, serves as one quantitative measurements of IBP activity (Fig. 1A) [29]. TH measurements are usually performed with a nanoliter osmometer, which allows researchers to monitor and record the freezing/melting temperatures of single ice crystals in IBP-containing solutions, under tightly controlled temperature conditions [30], while observing the shape of the ice crystals. Based on their TH activity, IBPs have been compared and classified in two main groups: moderately active IBPs, exhibiting TH in the range of 0–2 °C, and hyperactive IBPs that can achieve these TH values at one-tenth the concentration, with upper limits of 2–13 °C [7].

The primary model used to describe the ability of IBPs to control ice crystal growth and shape was proposed by Raymond and DeVries [26]. This is the adsorption-inhibition mechanism. According to this mechanism, the adsorption of IBPs to ice induces surface micro-curvatures between bound IBPs, making any further addition of water molecules to the ice surface energetically unfavourable when a critical radius is reached, as described by the Gibbs–Thomson

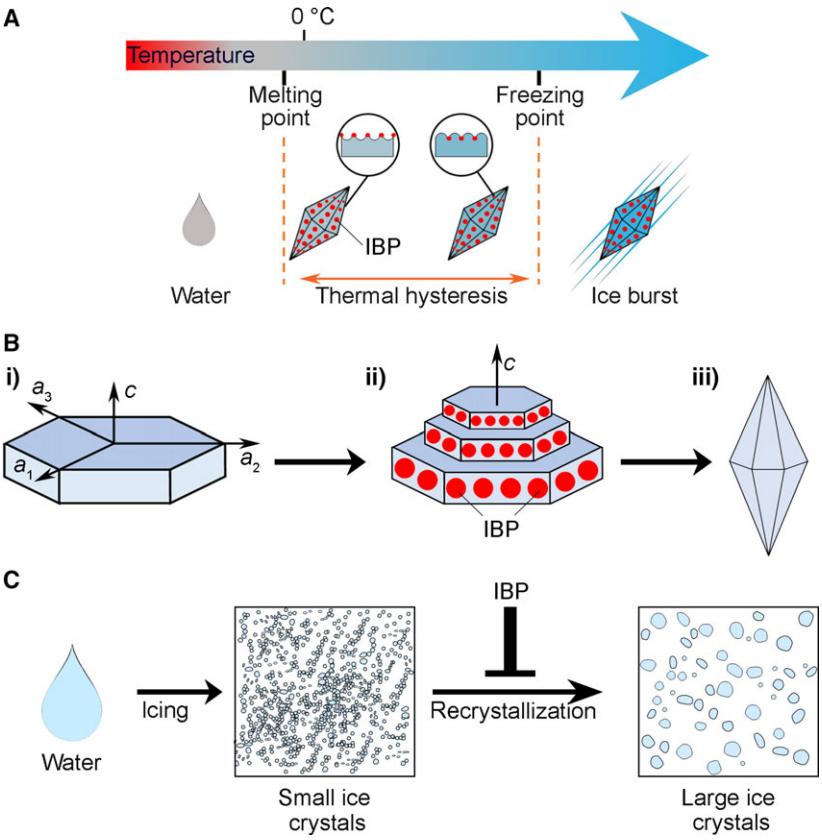

Fig. 1. Activities of IBPs. (A) TH. The adsorption of IBPs to the ice surface induces the lowering of the water freezing point and the raising of the ice melting point. At temperatures below the freezing point, it is possible to observe the growth of ice crystals in an explosive manner (ice burst). (B) Ice shaping. The morphology of ice crystals is strictly related to the ability of an IBP to bind one or more specific ice crystal planes. The hexagonal ice unit (i) is defined with *a* and *c* axes. The basal plane of the ice crystal is coloured blue, while the prismatic planes are light blue. IBPs bound to prismatic planes inhibit ice growth along the *a*-axes (ii), generating hexagonal bipyramid ice crystals (iii). (C) IRI. IBPs stabilize small ice crystals and inhibit their growth into larger ones. IBPs are indicated as red spheres.

equation. Therefore, the presence of IBPs strongly influences the growth kinetics of selected ice crystal faces, depending on the affinity of the various IBPs for the different ice crystal faces (Fig. 1B). Since the morphology of a crystal is dominated by its slowest growing face, a deviation in the growth kinetics of the various crystal faces results in a change in morphology. For instance, most moderately active IBPs bind to prismatic and/or pyramidal planes, and rarely to the basal plane, giving rise to a bipyramidal ice shape that forms along the *c*-axis during crystal growth slightly below the equilibrium freezing point [31]. In contrast, hyperactive IBPs bind rapidly to the basal plane – as well as some combination of prismatic or pyramidal planes – to cause a flattening or rounding of the two hexagonal bipyramidal tips due to suppression of growth along the *c*-axis [31,32].

Apart from TH, an additional metric for categorizing IBPs is by their IRI activity [33]. IRI also uses the adsorption–inhibition mechanism to stabilize small ice crystals and prevent loss of their water into larger crystals (Fig. 1C) [16,34]. IRI activity can be measured by forming thin layers of ice and optically monitoring the size of ice grains in the presence of different IBP concentrations over time. Several methods have been developed in the past 30 years. (a) The so-called 'splat assay' deposits water droplets from a height of > 1 m onto an ultracold metal surface to attain thin wafers of ice grains, the mean dimensions of which are quantified before and after a set amount of time to measure IRI [35]. By performing splat assays on serial dilutions of an IBP, the IBP's threshold concentration for retaining IRI can be determined and compared to other proteins [36]. (b) The 'sandwich assay' is a variation of the splat method done in high sucrose concentrations, where multiple ice crystals are surrounded by solvent and sandwiched between two glass plates. Ice crystal size is monitored during a set time and analysed to extract the rate constant for ice recrystallization. The inhibitory concentration (C_i; i.e. the concentration causing 50% inhibition of ice recrystallization) is calculated by plotting the rate constant as a function of IBP concentrations [37]. Unfortunately, data obtained from the two assays are not directly comparable due to differences in sample composition and assay conditions [9]. Based on C_i values from the sandwich assay, IBPs have been classified as: very effective ($C_i < 10^{-1}$ μmol·L^{-1}), effective ($10^{-1} < C_i < 10^3$ μmol·L^{-1}) and ineffective ($C_i > 10^3$ μmol·L^{-1}) [38].

To date, all IBPs with TH activity show IRI but there is not yet an understanding of how these activities scale, nor how they directly relate to ice shaping [39]. For example, plant IBPs typically have weaker TH activities than fish AFPs [32,40] but have higher IRI activity [17,41]. Also, IBPs can be diluted beyond the point of measurable TH, yet still present distinct ice shaping and IRI. What makes deciphering trends in relative activity more difficult is that measurements of both TH and IRI activities of different IBPs, and their ice shaping properties, are affected by several experimental variables. This is particularly true for TH measurements where the holding temperature and cooling rate used, the solute concentration, the type of IBP present in solution, the initial ice crystal size and the IBP concentration all influence the result [42–44]. The lack of standardization can make it difficult to compare absolute activity values between laboratories, although within an experimental regime, values are reproducible and comparable. Instigating a set of more stringent parameters that are maintained between research groups will be necessary for the universal, activity-based classification of IBPs.

Ice-binding sites and their identification

Thermal hysteresis and ice recrystallization both require IBPs to bind to ice. There have been several theories over the years about how IBPs, which are freely soluble in liquid water, are able to recognize and adsorb to ice, the solid state of water. It is now accepted that each IBP has one specific area through which it binds ice. These surfaces are known as the ice-binding sites (IBS) and are typically flat and relatively hydrophobic, with the most active IBPs often containing a repetitive motif that is threonine-rich (e.g. T-X-T and T-X-N) [7,10]. The presence of this motif can make identifying the IBS easier, although it is missing altogether from some IBPs. One approach to IBS identification is based on this site being the most highly conserved surface of the IBP, and combining sequence (i.e. multiple alignment with orthologs), 3D structure information and computational simulations [e.g. ice docking and molecular dynamic (MD) simulations]. The putative IBS can then be confirmed by rational-design mutagenesis to substitute supposed ice-binding residues with large, bulky residues that would spoil the IBS (e.g. Tyr), followed by functional analysis to identify mutations that drastically decrease TH activity. To date, this labour-intensive approach has correctly identified the IBSs of most IBPs, including type III AFP [45], *Lp*IBP from *Lollium perenne* [40] and *Marinomonas primoryensis* IBP (*Mp*IBP) from *M. primoryensis* [46].

Structure-based classification of IBPs

To date, the solved structures of IBPs belong to 11 recognizably different folds [10] and additional structures are being processed for publication (Fig. 2). This amazing diversity of IBP structures has evolved across different Kingdoms of life to serve the same function: controlling ice growth. An early attempt was made to classify IBPs isolated from fishes into four different groups according to their 3D structures: antifreeze glycoproteins (AFGPs) and three AFP types [47]. The structure of type I AFP is an alanine-rich α-helix [48], whereas type II and III AFP from fishes are small globular proteins of different origins [49,50]. Interestingly, while these different types of AFPs are prime examples of convergent evolution to serve the same function, several of the types evolved independently in different species, maintaining both the same function and structure. For instance, the AFGPs evolved independently in Antarctic and Arctic fishes as polymers of a simple glycosylated tripeptide repeat [51]. Additionally, the type I AFPs independently arose at least four times in different fishes [52].

Outside of fishes, the diversity of IBP types has defied such tidy classifications, although the β-solenoid fold is common. Several insect IBPs are β-solenoids stabilized by extensive disulphide bridges, e.g. the IBP

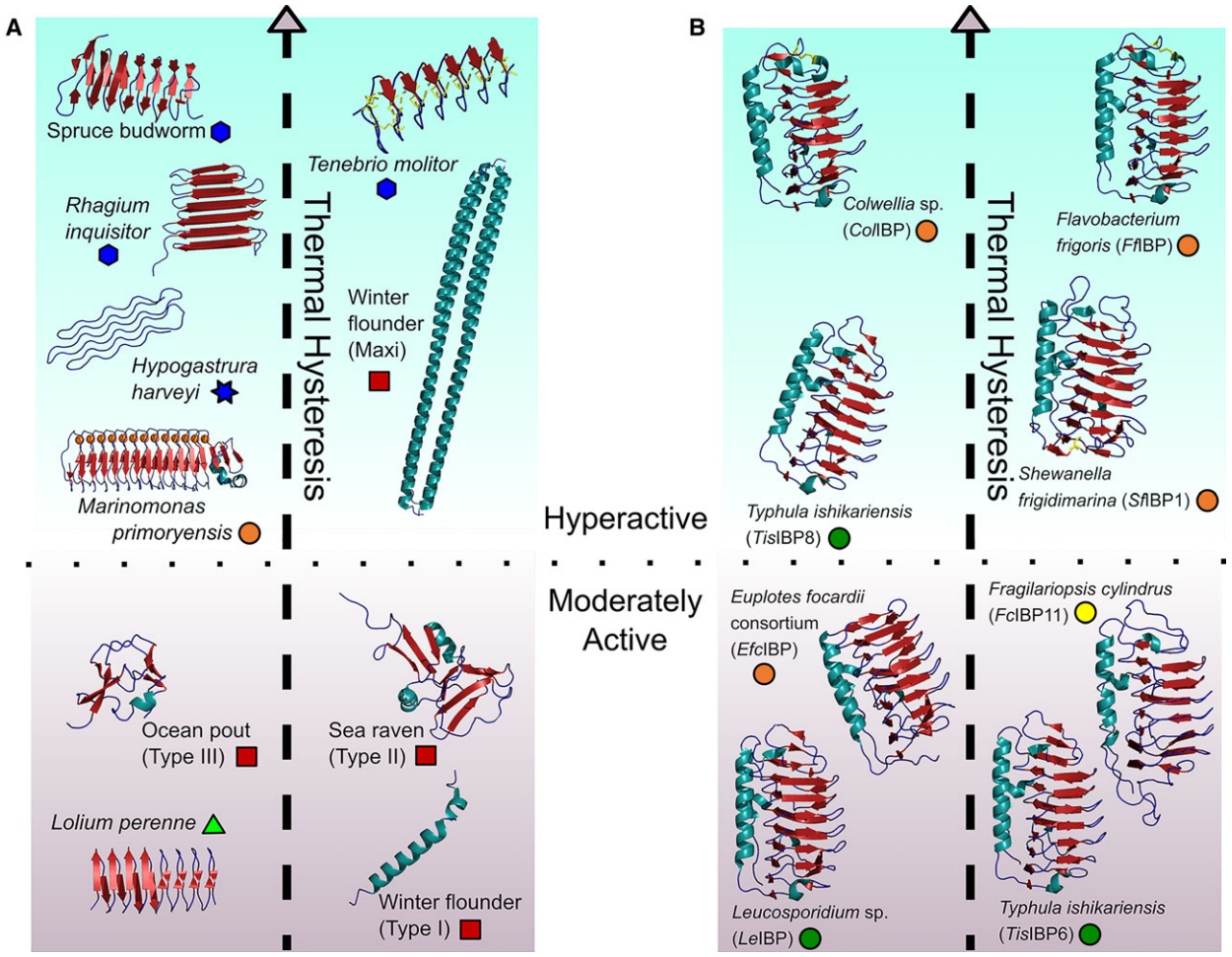

Fig. 2. Overview of IBP structures and their corresponding ice-binding activity. The structures of IBPs, both non-DUF3494 (A) and DUF3494 (B), are aligned along a vertical axis of TH. IBPs demonstrating higher TH activity are placed above those with lower activities; a rough break between hyperactive and moderately active IBPs is shown. Structures are coloured by secondary structure, with helices shown in teal, beta sheets shown in red, and loops shown in dark purple. Calcium ions are shown as orange spheres, and the disulphide bonds in TmAFP and several DUF3494 IBPs are coloured yellow. Symbols indicating phylogenetic groupings are found beside the species name, with red squares for fishes, green triangles for plants, blue hexagons for insects, blue stars for arthropods and circles for microorganisms (orange: bacteria, yellow: microalgae, green: fungi).

isoforms from *Tenebrio molitor* [53], *Rhagium inquisitor* [54] and spruce budworm [55]. In plants, *L. perenne* – also known as winter ryegrass – uses a β-solenoid moderately active IBP to mitigate freeze damage [40,56]. In microorganisms, the fold of the ice-binding domain of *Mp*IBP consists of a large β-solenoid that requires calcium ions to fold properly [46,57]. Indeed, the prevalence of the β-solenoid in IBPs has led to the hypothesis that the particular spacing of Thr residues along the helical-axis of the solenoid is optimal for matching ice on the basal and prism planes [53].

Despite these many IBPs that use a β-solenoid shape to achieve ice-binding activity, there are still examples of completely different folds. For example, the IBP from the primitive arthropod *Hypogastrura harveyi* has the remarkably different fold of a bundle of polyproline type II coils [58,59]. Even among the different β-solenoid-containing IBPs mentioned above, significant differences exist in length, cross-section shape and diameter, repetitive motifs and stabilizing interactions through disulphides or metals. The distinct tertiary structures taken up by IBPs has undoubtedly played a part in the differences in TH activity on display (Fig. 2A).

However, there is one IBP fold of distinction. The fold in question is a discontinuous β-solenoid (Fig. 3), first introduced by two 3-D structures solved in 2012 [60,61]. The signature domain of this fold, originally called IBP-1, is designated by the Pfam library [62] as the domain of unknown function (DUF) 3494. What makes this IBP fold so remarkable is less its discontinuous structure – which is interesting into and of itself – but rather the observation that DUF3494 proteins are commonly found among bacteria, yeasts, fungi and microalgae in an apparent example of lateral gene transfer, as opposed to the convergent evolution that gave rise to most other IBPs [42,63–66]. Also, of great interest is that, despite their common structure, the characterized proteins endowed with the IBP-1 fold exhibit a wide range of IBP activity (Fig. 2B). In this review, we will include the current state of research pertaining to DUF3494-containing IBPs, which will be referred to as DUF3494 IBPs.

The DUF3494 protein family

A protein domain represents a functional and structural unit. Currently, 20% of all protein domains lack an attributed function, hence the annotation as domains of unknown function (DUFs) in the Pfam database [62]. DUFs are widespread in all phyla, but most of them belong to bacteria (ca 2700 DUFs), while 1500 DUFs are from eukaryotes. Despite the unknown function of these domains, many are highly conserved, indicating a key biological role [67].

DUF3494s are typically found in psychrophilic organisms, prevalently bacteria belonging to the phyla of *Flavobacterium* and *Bacteroidetes* [68]. In some cases, the DUF3494 fold is associated with an N-terminal signal peptide and with the secretion domain T9SS typical of *Bacteroidetes* extracellular proteins [69]. Other DUF3494-containing proteins were also found in yeasts, algae, fungi and even archaea from regions that experience cold temperatures. In the last decade, increasing numbers of proteins containing the DUF3494 were demonstrated to bind ice crystals and, hence, were classified as IBPs [21,60,70–77]. The current number of DUF3494 proteins confirmed as IBPs is so large that it raises the

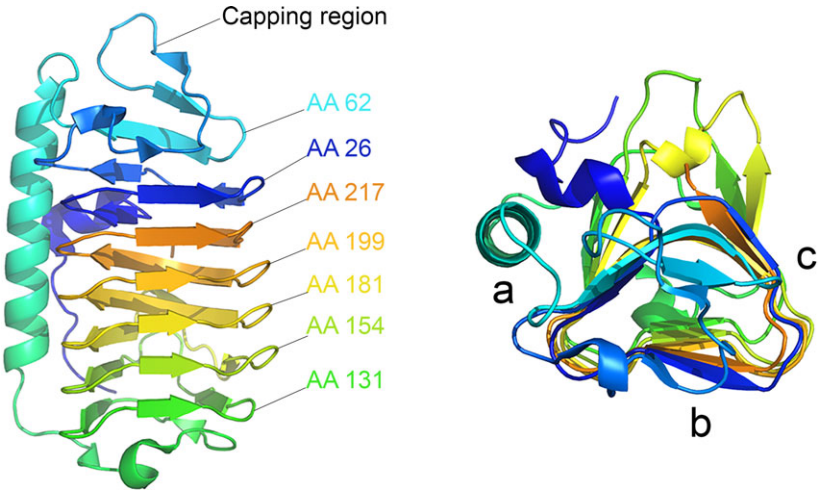

Fig. 3. 3D structure of *Tis*IBP6. 3D structure of *Tis*IBP6 (PDB code: 3VN3) has been used as example of the structure of DUF3494 IBPs. The protein is coloured in chainbow format, the faces of β-solenoid are indicated with the letters a, b and c. Residue numbers at equivalent points in each coil of the solenoid are presented.

question of whether or not there are DUF3494s that do not bind to ice.

Architecture of DUF3494 IBPs

Based on the Pfam library, 865 proteins are predicted to contain the DUF3494 (accession: November 2018). These proteins are arranged into 84 architectures, with the single-DUF3494 architecture (Fig. 4A) being the most representative (~ 68%). Almost all characterized DUF3494 IBPs exhibit this simple architecture [60,72–74,78–81]. Generally, single-DUF3494 IBPs also contain an N-terminal signal peptide, suggesting that these proteins are secreted into the environment near the cells or accumulate in the membrane [24,25].

Currently, only two IBPs belonging to different DUF3494 architectures have been biochemically characterized. The first is IBPv, from the *Flavobacteriaceae* strain 3519–10 isolated from the Vostok lake [75,82]. This protein contains two consecutive DUF3494 domains, connected by a 17-residue linker and ending with a short C-terminal domain (Fig. 4B). Additional uncharacterized proteins with tandem copies of the DUF3494 are present in the Pfam library, such as the archaeal protein from *Methanoregula boonei* that houses five such repeats. The second example is the multidomain *Sf*IBP_1 from *Shewanella frigidimarina*. This protein contains a single DUF3494 preceded by an N-terminal series of tandem bacterial immunoglobulin-like (BIg) domains (Fig. 4C). Though the first example to be characterized, this architecture is not unique to *Sf*IBP_1; many DUF3494-containing proteins having been partnered with varying numbers of BIg domains.

There are numerous other DUF3494-containing architectures, some that include alternative localization domains like the Autotransporter domains associated with the Type V Secretion System [83], or the Gram-positive Anchor domain [84]. Meanwhile, other companion architectures encompass sugar-interacting modules, like the PA14 and Laminin G3 domains (Fig. 4D). As there are no current characterized exemplar proteins for these architectures, it is unclear whether these proteins have ice-binding activity, and – if so – how the additional domains help to facilitate the proteins' functions.

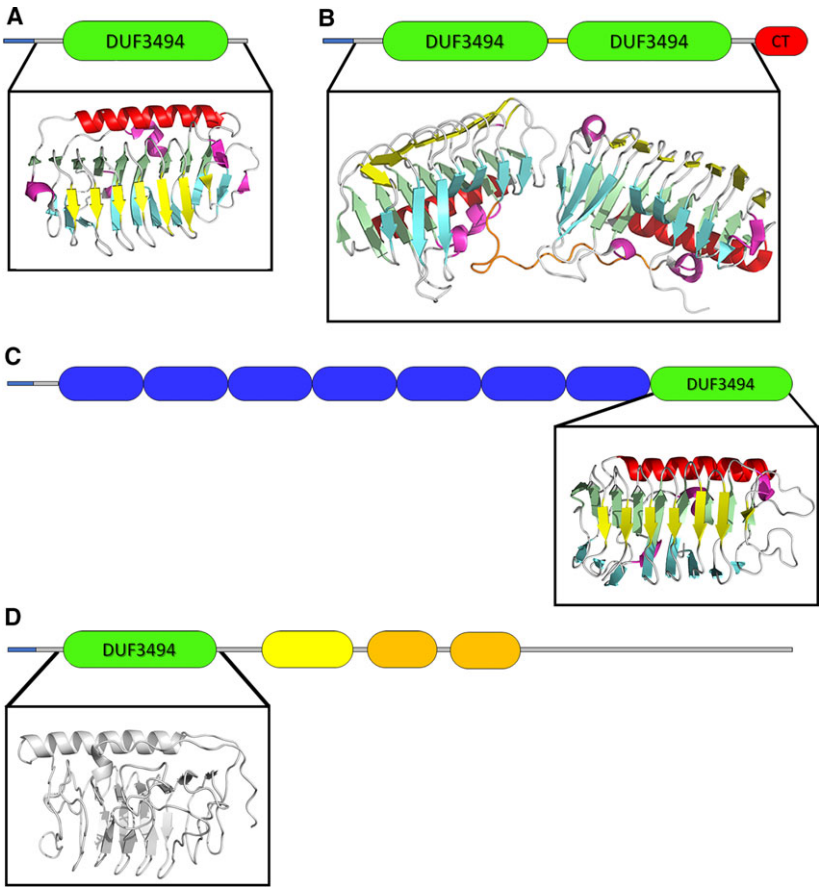

Fig. 4. Architectures and 3D structures of DUF3494 IBPs. (A) Single DUF3494 domain architecture. Boxed is the 3D structure of *Tis*IBP6 (PDB code: 3VN3). (B) Architecture of double-domain DUF3494 IBP: two DUF3494 elements are connect by a 17-residue linker (in orange), the C-terminal domain is in red; the 3D structure of IBPv (PDB code: 5UYT) is boxed. (C) Architecture of a multidomain DUF3494 IBP: BIg domains are coloured in blue, whereas the black box contains the 3D structure of *Sf*IBP_1 (PDB code: 6BG8). (D) Architecture of DUF3494 domain associated with sugar-interacting domains: Laminin G3 domain is coloured in yellow, while PA14 domains are in orange. The black box contains the 3D structural model of the DUF3494 domain predicted by i-TASSER [115]. In all architecture representations, the N-terminal signal peptide is coloured in light blue. In all 3D structures, β strands belonging to the a, b and c faces of β-solenoid are in green, yellow and cyan, respectively. The helix α1 is in red and the 3_{10} helices in magenta. The 3D model is in grey.

Biological role of DUF3494 IBPs

The DUF3494 IBPs have been found in many organisms from a variety of habitats, including seas, lakes, glaciers, sea-ice and snow-covered fields [14,25,71,85]. While these can be harsh environments, biodiverse communities of microorganisms can still thrive, provided they are outfitted with the proper survival strategies. One such strategy for microorganisms living in sea-ice is the production in large quantities of IBPs [42,66]. Most DUF3494 IBPs are predicted to have a signal peptide and therefore to be secreted from the cells into the surrounding medium. However, the role of IBPs in sea-ice is still unclear. It has been proposed that IBPs modify the structure of brine channels that naturally form in sea-ice. By attaching to the icy walls of the channels the IBPs may make them more convoluted, therefore decelerating brine drainage from the sea-ice layer and increasing the habitable space (Fig. 5A) [22,23,42]. Indeed, several species of fungi, bacteria and diatoms have been confirmed to secrete their DUF3494 IBPs into the growth media, from where they could work to carve out a niche for their host organisms in the ice [14,42,86].

Alternatively, secreted DUF3494 IBPs could be used to prevent ice recrystallization in the immediate vicinity of the organism, thereby promoting survival through decreased risk of cell damage. Evidence of this behaviour was reported by James Raymond, who found that the ability of an aquatic moss, *Byrum argenteum*, to survive subzero temperatures was due to the accumulation of DUF3494 IBPs on its surface. Interestingly, the metagenomic analysis revealed that the IBPs were actually being secreted from epiphytic bacteria living on the moss, providing an interesting example of IBP-mediated symbiosis (Fig. 5B) [24].

While many DUF3494 IBPs have explicit export signal peptides, others contain a lipobox signal peptide, which associates the protein with the cell membrane. One such example is the earlier described *Sf*IBP_1, which has been confirmed through immunoblotting to be membrane-associated [72]. A potential reason for this localization can be gleaned from examining the IBP of *M. primoryensis* (*Mp*IBP), another example of a membrane-associated IBP expressed by an Antarctic marine bacterium. This 1.5-MDa protein encompasses multiple domains, including many tandem BIg domains reminiscent of those found in *Sf*IBP_1. The BIg repeats separate an N-terminal membrane-anchoring region from several C-terminal domains that allow the bacterium to bind to both ice and the diatoms [19]. The architecture of *Mp*IBP allows it to function as an ice adhesin, adhering its bacterial host to surface ice in its aquatic environment, while also promoting connections with phototrophic diatoms. In doing so, *M. primoryensis* is able to remain in the upper oxygen-rich strata of its environment, connected to nutrient-producing diatoms. Recent studies have proposed that *Sf*IBP_1, which possesses a similar architecture (i.e. BIg domains and a membrane-anchoring mechanism), could function

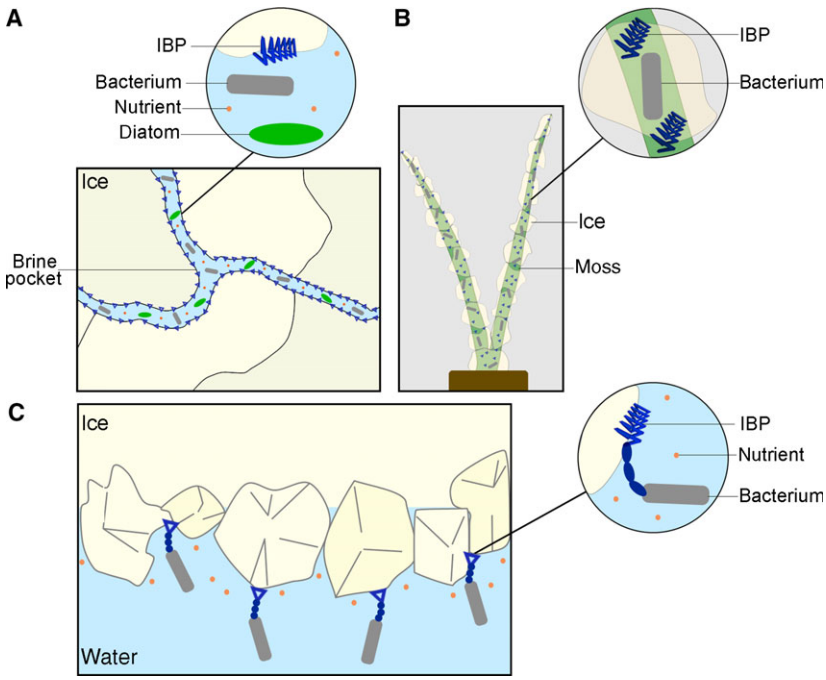

Fig. 5. Biological roles of DUF3494 IBPs. (A) Secreted DUF3494 IBPs stabilize brine channels (or brine space) to maintain a liquid environment near the cells. (B) Symbiosis between the aquatic moss, *Byrum argenteum* and epiphytic bacteria living on its surface. DUF3494 IBPs are secreted from bacteria and accumulate on the moss surface protecting it from freezing damage [24]. (C) *Sf*IBP_1 from *Shewanella frigidimarina* is anchored to the cell membrane and promotes adhesion between the bacteria and the ice surfaces [72].

as a new type of ice adhesin (Fig. 5C). While no other DUF3494 proteins have been found to share this property as of yet, the many similarly organized DUF3494-containing proteins found in the Pfam library indicate that ice adhesion may be a more prevalent strategy for surviving cold aquatic environments than previously thought [19,72].

Evolution of DUF3494 IBPs

Convergent evolution of both structure and function cannot explain the distribution of DUF3494 IBPs, which crosses several taxonomic divides. It is highly unlikely that the complex tertiary structure of DUF3494 (Fig. 3) that includes a beta-solenoid joined together from opposite ends of the protein could be reinvented from a different progenitor to bind ice. Phylogenetic analyses of DUF3494 IBPs have been undertaken by several research groups, using both large and small cohorts to deduce the evolutionary history of these proteins [42,63–66]. The most notable trend observed is that DUF3494 IBPs from wildly different organisms cluster together. The phylogenetic tree in which fungal, algal and bacterial DUF3494 IBPs show higher sequence similarity to each other than to other IBPs within their respective Kingdoms, as also confirmed in a recent work published by Arai and collaborators [87] (Fig. 6). Indeed, the bacteria *S. frigidimarina* and *Flavobacterium frigoris* even provide examples of multiple DUF3494 IBP-encoding genes within the same organism – even found directly beside each other in the genome – that group differently on the phylogenetic tree [42,64,72].

The most likely explanation for the distribution of DUF3494 IBPs is horizontal gene transfer (HGT). HGT is the passing of genetic material 'horizontally' between organisms, as opposed to 'vertically' between generations [88]. Precedence for IBP-related HGT exists as the best explanation for the distribution of type II lectin-like AFP, found in several phylogenetically distinct families of fishes [89]. Sea-ice can be regarded as a 'hot spot' for HGT [90]. Studies showed that extracellular DNA in brine is enriched up to 13 times compared to the under-ice ocean [91] and that HGT is higher at the solid–liquid interface than in the liquid phase [92]. The high density of potential donor and recipient organisms within brine channels and the solid icy walls of the channels, which may act as a stabilizing substrate for attached DNA, possibly make sea-ice a favourable environment for HGT [21]. By comparing the phylogenetic tree of DUF3494 IBPs with that of small subunit (SSU) rRNA speciation markers, Sorhannus has identified at least four occurrences of horizontal transfer of DUF3494 IBP genes [63]. Two of these incidents occurred between eukaryotes, such as the diatom *Chaetoceros neogracile* transferring its DUF3494 IBP gene to the copepod *Stephos longipes* [63,93], while the other two occurred between prokaryotes as in the case of the proteobacterium *Polaribacter irgensii* that transferred its DUF3494 gene to four proteobacteria (*Shewanella denitrificans*, *Shewanella frigidamarina*, *Colwellia* sp., *Psychromonas ingrahamii*) [63]. HGT events from prokaryote to eukaryote would likely be less frequent due to the differences in promoter regions and in codon usage [94]. Nevertheless, a recent work suggests an HGT occurred from a bacterium to the Antarctic fungus *Antaromyces psychrotrophicus* [87].

While HGT provides a solid hypothesis that explains the distribution of DUF3494 IBPs, an alternative explanation cannot be entirely ruled out. The differences between the SSU rRNA and DUF3494 IBP trees could also be explained by rampant gene duplication in progenitor species, followed by subsequent loss of gene copies further along the evolutionary timeline [64,95]. However, the sheer number of gene duplication and loss events necessary to fully explain the evolution of this widespread protein makes this explanation unlikely.

Activity of DUF3494 IBPs

Thermal hysteresis activity

The IBPs belonging to the DUF3494 family possess a wide range of TH activities (Fig. 2B and Table 1), with values ranging from 0.08 °C (at 200 μM of Afp4 from *Glaciozyma antarctica*) [76] to 3.8 °C [at 140 μM of *Colwellia* sp. strain SLW05 IBP (*Col*IBP)] [74]. Although these measurements were carried out in

Fig. 6. Phylogenetic analysis of DUF3494 IBPs. Phylogenetic trees based on (A) amino acid sequences of DUF3494 IBPs, and (B) 16S or 18S ribosomal RNA (B). The bootstrap values are coloured in black and red on the basis of maximum likelihood and Bayesian inference methods. Proteins with confirmed ice-binding activity are underlined. The colours of symbol contours indicate the bacterial phyla: Proteobacteria (black), Planctomycetes (green), Firmicutes (cyan), Actinobacteria (orange) and Bacteroidetes (purple); and algae phyla: *Bacillariophyta* (black), *Haptophyta* (magenta) and *Chlorophyta* (cyan). Reproduced from Ref. [87], with minor changes.

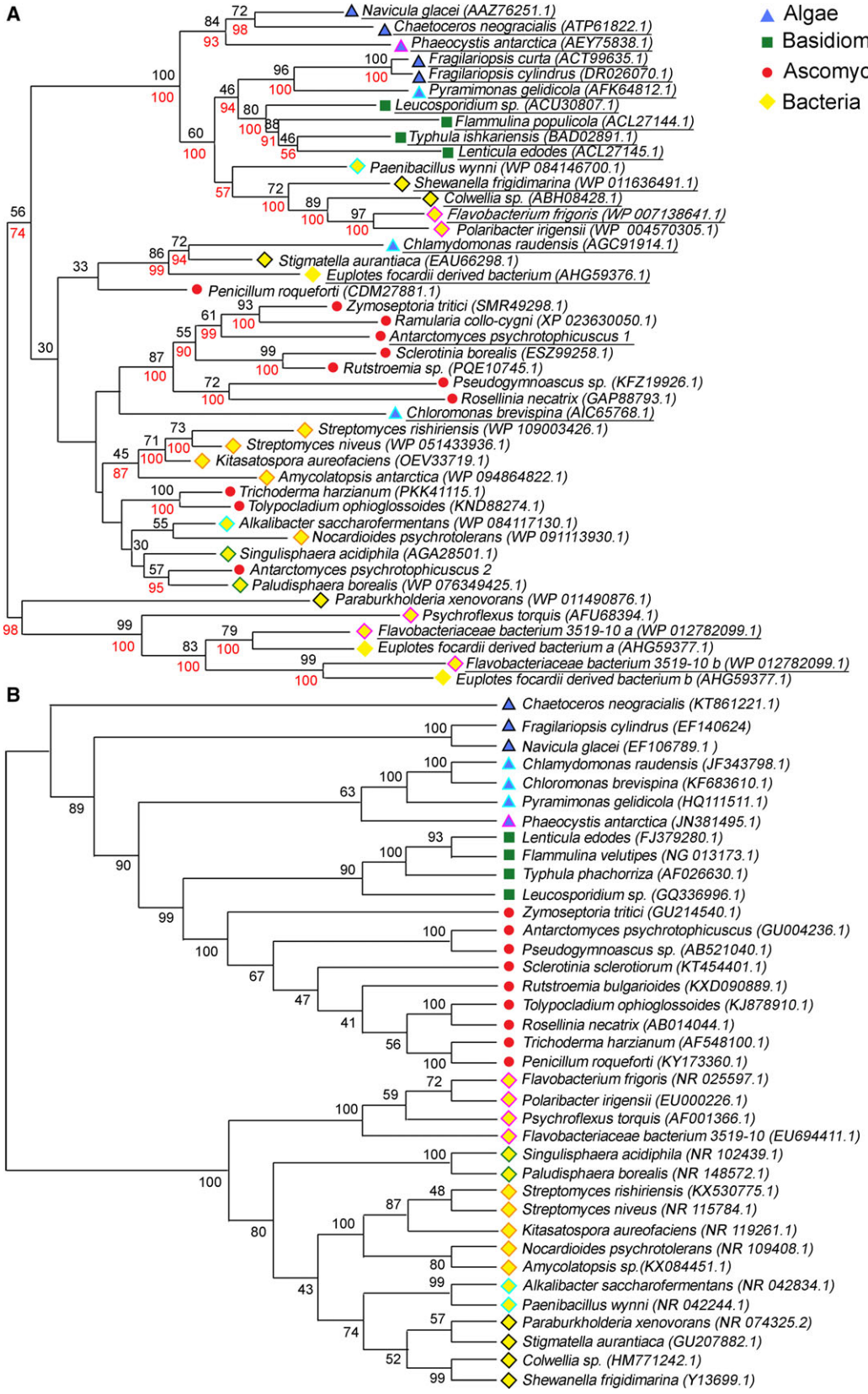
A
Algae
Basidiomycete
Ascomycete
Bacteria
Navicula glacei (AAZ76251.1)
Chaetoceros neogracialis (ATP61822.1)
Phaeocystis antarctica (AEY75838.1)
Fragilariopsis curta (ACT99635.1)
Fragilariopsis cylindrus (DR026070.1)
Pyramimonas gelidicola (AFK64812.1)
Leucosporidium sp. (ACU30807.1)
Flammulina populicola (ACL27144.1)
Typhula ishkariensis (BAD02891.1)
Lenticula edodes (ACL27145.1)
Paenibacillus wynni (WP 084146700.1)
Shewanella frigidimarina (WP 011636491.1)
Colwellia sp. (ABH08428.1)
Flavobacterium frigoris (WP 007138641.1)
Polaribacter irigensii (WP_004570305.1)
Chlamydomonas raudensis (AGC91914.1)
Stigmatella aurantiaca (EAU66298.1)
Euplotes focardii derived bacterium (AHG59376.1)
Penicillum roqueforti (CDM27881.1)
Zymoseptoria tritici (SMR49298.1)
Ramularia collo-cygni (XP 023630050.1)
Antarctomyces psychrotophicuscus 1
Sclerotinia borealis (ESZ99258.1)
Rutstroemia sp. (PQE10745.1)
Pseudogymnoascus sp. (KFZ19926.1)
Rosellinia necatrix (GAP88793.1)
Chloromonas brevispina (AIC65768.1)
Streptomyces rishiriensis (WP 109003426.1)
Streptomyces niveus (WP 051433936.1)
Kitasatospora aureofaciens (OEV33719.1)
Amycolatopsis antarctica (WP 094864822.1)
Trichoderma harzianum (PKK41115.1)
Tolypocladium ophioglossoides (KND88274.1)
Alkalibacter saccharofermentans (WP 084117130.1)
Nocardioides psychrotolerans (WP 091113930.1)
Singulisphaera acidiphila (AGA28501.1)
Antarctomyces psychrotophicuscus 2
Paludisphaera borealis (WP 076349425.1)
Paraburkholderia xenovorans (WP 011490876.1)
Psychroflexus torquis (AFU68394.1)
Flavobacteriaceae bacterium 3519-10 a (WP 012782099.1)
Euplotes focardii derived bacterium a (AHG59377.1)
Flavobacteriaceae bacterium 3519-10 b (WP 012782099.1)
Euplotes focardii derived bacterium b (AHG59377.1)
B
Chaetoceros neogracialis (KT861221.1)
Fragilariopsis cylindrus (EF140624)
Navicula glacei (EF106789.1)
Chlamydomonas raudensis (JF343798.1)
Chloromonas brevispina (KF683610.1)
Pyramimonas gelidicola (HQ111511.1)
Phaeocystis antarctica (JN381495.1)
Lenticula edodes (FJ379280.1)
Flammulina velutipes (NG 013173.1)
Typhula phachorriza (AF026630.1)
Leucosporidium sp. (GQ336996.1)
Zymoseptoria tritici (GU214540.1)
Antarctomyces psychrotophicuscus (GU004236.1)
Pseudogymnoascus sp. (AB521040.1)
Sclerotinia sclerotiorum (KT454401.1)
Rutstroemia bulgarioides (KXD090889.1)
Tolypocladium ophioglossoides (KJ878910.1)
Rosellinia necatrix (AB014044.1)
Trichoderma harzianum (AF548100.1)
Penicillum roqueforti (KY173360.1)
Flavobacterium frigoris (NR 025597.1)
Polaribacter irigensii (EU000226.1)
Psychroflexus torquis (AF001366.1)
Flavobacteriaceae bacterium 3519-10 (EU694411.1)
Singulisphaera acidiphila (NR 102439.1)
Paludisphaera borealis (NR 148572.1)
Streptomyces rishiriensis (KX530775.1)
Streptomyces niveus (NR 115784.1)
Kitasatospora aureofaciens (NR 119261.1)
Nocardioides psychrotolerans (NR 109408.1)
Amycolatopsis sp.(KX084451.1)
Alkalibacter saccharofermentans (NR 042834.1)
Paenibacillus wynni (NR 042244.1)
Paraburkholderia xenovorans (NR 074325.2)
Stigmatella aurantiaca (GU207882.1)
Colwellia sp. (HM771242.1)
Shewanella frigidimarina (Y13699.1)

Table 1. TH activity of DUF3494 ice-binding domains.

Protein ID	Organism	TH activity	Molecular weight (kDa)	Reference
Afp4	*Glaciozyma antarctica*	0.08 °C at 200 μM	25.3	[76]
*Anp*IBP1	*Antarctomyces psychrotrophicus*	0.56 °C at 150 μM	21.4	[87]
*Cn*IBP	*Chaetoceros neogracile*	0.80 °C at 40 μM	26.2	[71]
*Col*IBP	*Colwellia* sp. strain SLW05	3.80 °C at 140 μM	24.4	[74]
*Efc*IBP	Bacterium consortium of *Euplotes focardii*	0.53 °C at 50 μM	23.4	[70]
*fc*IBP11	*Fragilariopsis cylindrus*	0.90 °C at 350 μM	25.9	[21]
*Ff*IBP	*Flavobacterium frigoris* PS1	2.50 °C at 50 μM	28.4	[78]
IBP*v*	*Flavobacteriaceae* bacterium 3519-10	2 °C at 50 μM	54.0	[75]
*Le*IBP	*Leucosporidium* sp. AY30	0.35 °C at 370 μM	26.2	[80]
*Nag*IBP	*Navicula glaciei*	3.20 °C at 1.6 mM	24.4	[77]
*Sf*IBP_1	*Shewanella frigidimarina*	2 °C at 80 μM	24.5	[72]
*Tis*IBP6	*Typhula ishikariensis*	0.32 °C at 140 μM	22.1	[73]
*Tis*IBP8	*Typhula ishikariensis*	2 °C at 180 μM	22.3	[60]

different buffers and ionic strengths, and are not directly comparable, it is unlikely that such a big disparity in activity can be explained by differences in laboratory protocols. These data suggest that DUF3494 IBPs naturally have a range of activities that would otherwise only be seen in one IBP type by targeted mutagenesis to decrease activity to different extents. Has this process occurred during evolution, and for what reasons? The functional diversity of bacterial DUF3494 IBPs is remarkable, especially if one considers that TH activity is generally dictated by IBP origin. For instance, insect IBPs are generally hyperactive, whereas fish AFPs are usually moderate [7].

Interestingly, DUF3494 IBP isoforms within the same species can have a wide range of TH activities, as in the case of isoforms 6 and 8 of *Tis*IBP from the snow fungus *Typhula ishikariensis*. Despite their high sequence identity (83.4%), the TH activities of *Tis*IBP6 and *Tis*IBP8 at 0.11 mM are 0.3 and 2.0 °C, respectively. It has been hypothesized that the secretion of multiple isoforms of *Tis*IBP with various levels of TH activity may allow the snow mould fungus to thrive in different habitats exposed to subzero temperature [60,73].

Ice plane affinity of DUF3494 IBPs

To help visualize the IBPs' binding planes, a fluorescence-based ice plane affinity (FIPA) analysis was developed [45,96], whereas other studies applied laser confocal fluorescence microscopy [22,97]. FIPA analysis, based on the traditional ice etching method [98] requires the use of fluorescently labelled IBPs, which are incorporated into a macroscopic single ice crystal hemisphere during its slow growth [98,99]. When testing hyperactive DUF3494 IBPs (e.g. *Tis*IBP8, *Col*IBP and *Sf*IBP_1), fluorescence was observed over the entire hemisphere, indicating that IBPs bind to multiple ice planes, including the basal plane [72–74]. Basal plane binding is a requirement for hyperactivity, but some IBPs with weak TH activity, like the *Lp*IBP from grass, also bind the basal plane [56]. Indeed, FIPA analysis of *Tis*IBP6 and *Euplotes focardii* bacterial consortium IBP (*Efc*IBP) showed that these moderate IBPs are able to bind basal and other planes [60,100]. This binding pattern to ice crystal planes was confirmed also for the moderate IBP isoform 11 from the sea-ice diatom *Fragilariopsis cylindrus* (*fc*IBP11) by laser confocal fluorescence microscopy of a single ice crystal in a solution of the fluorescently labelled protein [22]. In addition to these experimental methods, MD simulations of *fc*IBP11 indicated that the protein can, at least partly, bind the primary prism and basal faces, despite its moderate activity [79].

Ice crystal shaping by DUF3494 IBPs

The binding of DUF3494 IBPs to diverse crystal faces, including the basal ones, is reflected in ice crystal shaping by these proteins. Studies on single crystals of 10–50 μm in diameter show that DUF3494 IBPs also produce different patterns of ice growth and burst (i.e. the rapid growth of ice crystals at temperature below the non-equilibrium freezing point) [14,22,72,74,78,80,100]. For instance, in the presence of the hyperactive *Sf*IBP_1 within the TH gap, ice crystals present hexagonal shape, (Fig. 7i) whereas the bursting occurs with a dendritic pattern perpendicular to the *c*-axis (Fig. 7ii). These combined features were found also in other hyperactive DUF3494 IBPs [*Flavobacterium frigoris* PS1 IBP (*Ff*IBP) and *Col*IBP] [72,74,78] and

overall are typical of hyperactive IBPs, which share the ability to bind the basal plane of ice [31]. On the other hand, in the presence of the moderate *Efc*IBP, ice crystals assume a hexagonal truncated trapezohedron shape and they burst perpendicular to the *c*-axis (Fig. 7A,C) [100]. Moreover, detailed studies on single crystals in the presence of the moderate *fc*IBP11 (Fig. 7B), clearly showed that this protein is able to suppress the crystal growth along the *c*-axis similarly to hyperactive IBPs [22]. Overall, these results suggest that the basal plane affinity is required for hyperactivity but is not yet sufficient to explain it.

Interestingly, according to present day knowledge, all moderate basal-binder IBPs share a β-solenoid structure [56,60,80,81], which is also common to hyperactive ones. This observation suggests that the affinity for the basal plane benefits from the regular spacing of amino acid residues provided by β-solenoid structure [46,53,55]. Explaining the rationale of hyperactivity is not straightforward, and this issue is still open. Experiments on ice-binding kinetics might help to understand the differences between hyperactive and moderate basal-binder IBPs. Kinetics experiments carried out on the moderately active *Efc*IBP indicate it binds ice crystals very fast when compared to the hyperactive sbwAFP from spruce budworm [100].

Inhibition of ice recrystallization activity

Unfortunately, the paucity of data concerning IRI activity of DUF3494 IBPs makes it difficult to detail trends in their behaviour. Interestingly, *Efc*IBP and *Sf*IBP_1 have observable IRI activity even when diluted down to 2.5 and 5 nM respectively [70,72]. Though the values were obtained with two different techniques, and are not directly comparable, they are both very high IRI activities when compared with other IBPs measured by the same techniques [38]. To date, all IBPs with TH activity show IRI, but there is not yet an understanding of how the two activities scale [39]. The TH and IRI activities of *Efc*IBP and *Sf*IBP_1 represent an example of the uncertainty in the TH–IRI relationship. Both possess relatively high IRI, yet *Efc*IBP is a moderate IBP (TH of 0.53 °C at 50 μM), whereas *Sf*IBP_1 is hyperactive (TH of 2 °C at 80 μM). Before making too much of this distinction, it will be necessary to assay both proteins under the same conditions.

The limited available data on the activity of DUF3494 IBPs do not allow for a general rule about the IRI of these proteins to be drawn. As more high-throughput methods of IRI analysis become available, a comprehensive examination of all known DUF3494 IBPs may elucidate such a rule in the future [101]. In addition, one cannot exclude that the discovery of new DUF3494 IBPs could disclose new combinations of TH, IRI and ice shaping activities, not previously described.

Structural features of IBPs belonging to DUF3494

Currently, nine crystal structures have been reported for DUF3494 IBP family members: *Tis*IBP6 [60],

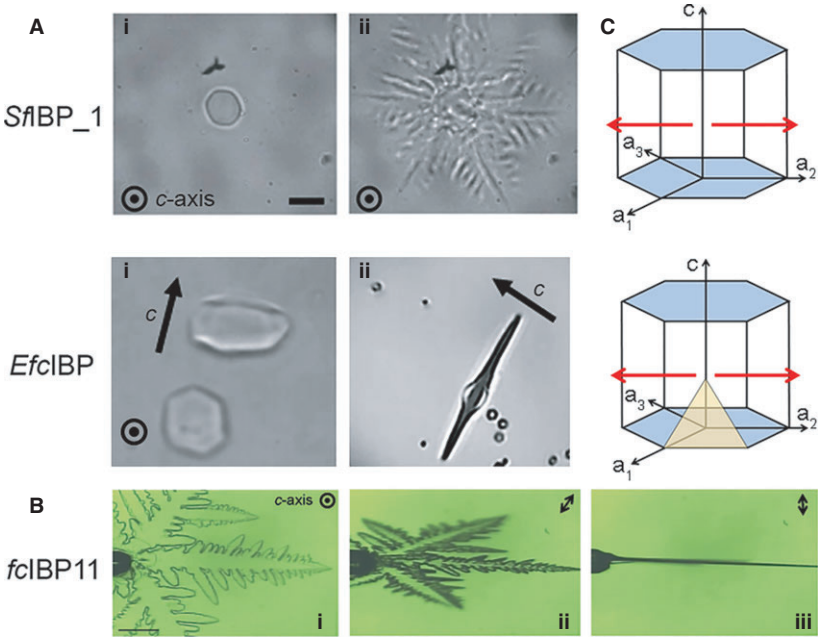

Fig. 7. Pattern of ice crystals shape and burst in the presence of DUF3494 IBPs. (A) Ice shaping in the presence of *Sf*IBP_1 and *Efc*IBP inside the TH gap (i) and at temperatures below the freezing point (ii) (B) The morphology of *fc*IBP11 at temperatures below the freezing point, observed by bright-field microscopy. The ice crystal was first visualized with the basal face parallel to the observation plane (i), then rotated by 45° (ii) and 90° (iii), to allow observation of the faces perpendicular to the basal face. (C) Model of hexagonal ice. The basal planes are coloured in light blue, while the pyramidal near basal plane are coloured in orange. Red arrows indicate the direction of the ice burst. Figure adapted from Refs. [72,100,22].

*Tis*IBP8 [73], *Leucosporidium* sp. AY30 IBP (*Le*IBP) [80], *Ff*IBP [78], *Col*IBP [74], IBPv [82], *Sf*IBP_1 [72], *Efc*IBP [81] and *fc*IBP11 [79]. All these proteins present the IBP-1 fold that consists of a discontinuous right-handed β-solenoid with a triangular cross-section formed by three parallel β-sheets (faces a, b and c), and an α helix that runs along the a-face, parallel to the main axis of the protein (Fig. 3). This extended α helix hides the a-face and prevents its exposure to solvent and, hence, to ice crystal surfaces, whereas the b- and the c-face are completely exposed to the solvent [60,73,74,78,80]. The discontinuity in the solenoid is optimally seen when the polypeptide sequence is coloured in chainbow format as illustrated in Fig. 3 for *Tis*IBP6. Here, adjacent red and blue coils of the solenoid come from distant regions (residues 26 and 217 respectively) of the polypeptide chain to form a seamless solenoid. This discontinuity is one of the features of the DUF3494 fold that would be difficult to duplicate in an independent evolution of the fold. It is also a reason why beta-solenoids are typically 'capped' to prevent end-to-end associations that can lead to amyloid formation [102,103].

The most divergent element between the structures is the 'capping region' at the N-terminal top of the β-solenoid. This element contains limited secondary structure and is located between two β-strands (Figs 3 and 8). Based on the general structure of the capping region, DUF3494 IBPs can be divided into three groups. The first group contains mostly bacterial IBPs (e.g. *Col*IBP, *Ff*IBP), where the cap is compact and held together by a disulphide bond [74,78]. The second group is much more structurally diverse, sporting two loops of varying lengths that interact with each other through varying residue contacts. Originally, this group was found only in eukaryotic IBPs (e.g. *Le*IBP, *Tis*IBP, *fc*IBP11), but the bacterial *Sf*IBP_1's capping structure was elucidated and shown to contain a superficially similar structure, albeit with very different residue contacts holding the loops together [60,73,74,78–80]. The final group currently includes only *Efc*IBP, which does not contain any capping structure (Fig. 8D). On the other hand, the bottom end of the DUF3494 solenoids (C-terminal) also has a capping structure. Far more consistent between DUF3494 IBPs, it usually folds as a small loop that cuts across the helix end and blocks the hydrophobic core. An exception is represented by *fc*IBP11, whose C-terminal capping sports a distinctly larger loop [79].

The role of the N-terminal capping region as a structural element is not completely understood, though its function is most likely related to protein stabilization. Considering the high propensity of

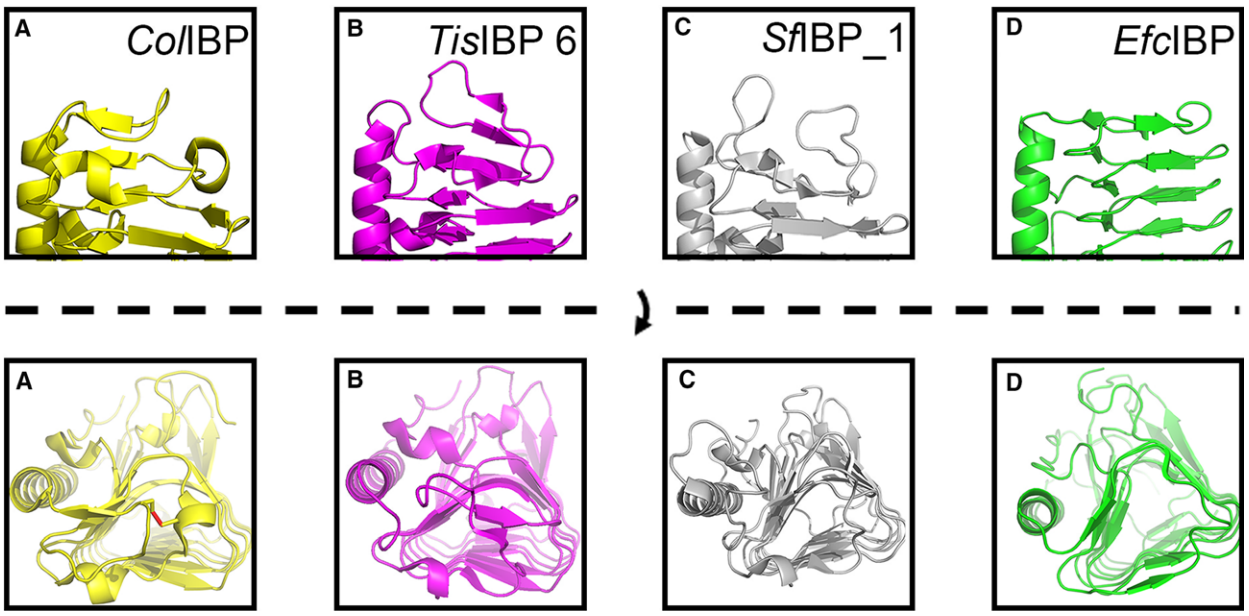

Fig. 8. Capping head region of DUF3494 IBPs. Lateral (top) and overhead (bottom) views of the capping head region for (A) *Col*IBP (PDB: 3WP9), (B) *Tis*IBP_6 (PDB: 3VN3), (C) *Sf*IBP_1 (PDB: 6BG8) and (D) *Efc*IBP (PDB: 6EY0). Based on the presence of capping head region, DUF3494 IBPs are classified in two groups. *Col*IBP, *Tis*IBP 6, *Sf*IBP_1 and *fc*IBP11 belong to the first group containing a capping head region. This region in *Col*IBP is stabilized by a disulphide bond (red in A). By contrast *Efc*IBP does not contain any capping region. Figure adapted from Ref. [72].

β-solenoid structures to form amyloids through fibril formation, cap regions are often a method for counteracting supramolecular head-tail linkage [104]. For example, removal of the cap from the pertactin β-solenoid protein lead to increased oligomerization and aggregation [103,105]. Many different forms of caps have been discovered, but all function by covering the hydrophobic core of the solenoid and interacting with unpaired hydrogen-bond donor/acceptors of the outermost β-strands. It is likely that the DUF3494 IBP capping regions are fulfilling a similar function, which makes the cap-less *Efc*IBP all the more interesting. The recombinant protein's monomeric and stable nature seems to contradict the capping structure's theoretical importance. However, there are β-solenoid proteins that use alternative strategies to prevent head-tail oligomerization. The *Escherichia coli* UDP *N*-acetylglucosamine acyltransferase protein (PDB: 1LXA) uses a combination of prolines and charged residues to deform the otherwise flat top of its beta-solenoid, thereby discouraging interaction [106,107]. Interestingly, a similar proline-induced bulge is present at the top of the *Efc*IBP solenoid, along with several smaller polar residues (Thr, His, Asn) that may also play a part.

The work of Do and coworkers also demonstrated the role of the S–S cap in thermal stability of *Ff*IBP, versus the more diffuse cap of *Le*IBP. Indeed, replacing the *Le*IBP cap with the S–S cap from *Ff*IBP improved the midpoint temperature (Tm) of the chimeric *Le*IBP by ~ 5 °C. The reciprocal cap exchange generated a chimeric *Ff*IBP lacking the disulphide bridge, which showed a lower Tm (~ 10 °C) [78]. Whether this difference in stability between groups 1 and 2 is true for all DUF3494 IBPs is unknown, as is the impact this stability has on function for proteins that are produced and work at low temperatures.

A peculiar architecture distinguishes the 3D structure of IBPv, which contains two IBP-1 homologous domains linked together [82]. The full-length protein has a TH activity of > 2 °C at concentrations higher than 50 μM, whereas the single domains exhibit much lower TH activity (0.40 and 1.37 °C at similar concentration for domains A and B, respectively) [75]. While differences in TH activity could be due to structural fragility – i.e. only the full-length protein can acquire the appropriate fold – duplication of the DUF3494 entails doubling the IBP's ice –binding surface and an increase in overall IBP size, both of which are known to increase the TH activity of IBPs [108–110]. Therefore, the duplication of DUF3494s may offer evolutionary advantages to microorganisms living at subzero temperatures.

Ice-binding sites (IBS) of DUF3494 IBPs

The DUF3494 IBPs seem to break most of the general rules about IBSs. The putative IBS of DUF3494 IBPs sports a variety of surfaces that differ greatly in composition. Structural biology and rational mutagenesis studies with the DUF3494 IBS have stressed the relevance of the b face of the β-solenoid in ice-binding, as well as of the loops that connect the a and b face [60,73,74,78,80]. An exception is *Efc*IBP, which can bind ice crystals through both b and c faces [81]. MD simulations with *fc*IBP11 have suggested other loops, not flat surfaces, like the α helix and the loop between the b- and the c-face, are involved in ice-binding [79]. By comparing these different surfaces, it may be possible to deduce what factors contribute to the disparity in activity between such structurally similar proteins.

A survey of data in the literature on structural and physical-chemical properties of IBSs leads to the following considerations:

- A comparison of IBS amino acid composition from DUF3494 IBPs of known structure and activity highlights the importance of hydrophobicity. For instance, the IBS of hyperactive *Tis*IBP8 is more hydrophobic than its moderate counterpart *Tis*IBP6 [73]. Indeed, mutation of the *Tis*IBP6 to include more hydrophobic residues resulted in an increase in TH activity. However, the content of threonine, hydrophobic and hydrophilic residues compared in hyperactive and moderately active DUF3494 IBSs does not generally show any clear trend.
- The topologies of the IBSs from the b face of several known structures (Fig. 3) seem to suggest that a flatter surface is more suitable to interact with the very regular surface of ice. Indeed, the hyperactivity of *Col*IBP was proposed to stem from its very flat IBS, a trait shared by *Ff*IBP but absent in the moderately active *Le*IBP and *fc*IBP11 [74,79]. However, counteracting this point is the rather flat surfaces of the moderately active *Tis*IBP6 and *Efc*IBP, and the rather uneven surface of the hyperactive *Sf*IBP_1. It appears that the qualitative trait of 'flatness' by itself may be too simple to account for such a complex interaction.
- The search for repetitive IBS motifs leads to an uncertain picture. Among the hyperactive DUF3494 IBPs, only *Ff*IBP contains a clear repetitive motif (T-A/G-X-T/N) [78] as seen in the hyperactive *Tm*IBP and *Mp*IBP [46,53]. Paradoxically, the moderately active *Efc*IBP

contains a similar repetitive motif (T-X-T or T-X-D) [81], which appears to rule out a preeminent role of repetitive motifs in the hyperactivity of DUF3494 IBPs.
- Molecular dynamic simulations carried out on *fc*IBP11 indicate it can bind both the basal and primary prism faces of the ice crystal [79]. This is in line with previous experimental results on this protein [22].

Overall, the mechanism of hyperactivity in DUF3494 IBPs remains elusive. This activity might depend not on single structural elements, but on their combination. As more DUF3494 IBP structures of varying levels of activity are solved, structure-activity relationships might become clearer.

Conclusions and perspectives

At the present, it is still unclear what structural attributes of IBPs determine their relative activity. The flatness and the regularity of IBS structure, the strength of ice interaction and its irreversibility, the ability to bind on a unique rather than multiple sides of an ice crystal are some of the arguments used to explain the diverse properties of IBPs. Taken together, the available data on the structure–function relationships of IBPs do not permit predictions about the activity of these proteins. Differences in IBP activity might be due to the various selective pressures exerted by different environments on IBP-producing organisms. Many research groups search for new IBPs that have specific traits (activity, ice shaping, stability etc.) amenable to biotechnology applications. However, the lack of a conserved IBP domain makes finding new examples labour-intensive, requiring the blind sampling of different species for activity followed by native purification of the protein for identification [111,112]. DUF3494 IBPs are an easy-to-find alternative, detectable through simple BLAST searches, allowing for recombinant expression for characterization.

Such a family of structurally similar proteins would appear uninteresting for research purposes, especially since the ease with which DUF3494 genes have been passed between microorganisms makes it seem less likely that new IBP structures will be discovered in these phyla. In insects, where IBP innovation from different progenitors is more feasible than HGT, there is likely to be much more diversity in structures. Indeed, three distinct IBP folds have already been discovered in insects [53–55] and on at least two occasions these folds have independently developed in unrelated insects through remarkable examples of convergent evolution [113,114]. Thus, within microorganisms the returns from prospecting for new IBP folds are likely to be minimal.

However, the appeal of DUF3494 IBP research is due to one of the most puzzling features of the DUF3494 fold members: the amazing range of TH activity they exhibit. The least potent members of this family are not even as strong in TH as plant IBPs, whereas the most potent are comparable in activity to insect IBPs. This range includes isoforms that are hyperactive with full suppression of growth out of the *c*-axis, others that also have growth suppression along the *c*-axis but low activity, and other moderate isoforms with full growth along the *c*-axis when TH is exceeded. Indeed, the large number of predicted DUF3494 IBP sequences are a relatively untapped resource of IBPs with diverse activities and biophysical characteristics, ready to be mined for potential uses in biotechnology. Furthermore, their sheer number and variety will provide more data points for solving the questions that still plague the IBP field, such as: (a) what is truly needed for a successful ice-binding surface? (b) Is there a predictable connection between intensity of TH and IRI activities? (c) How do IBPs evolve to gain/lose function within different environments/species?

It is still not known if all DUF3494 are IBPs. One could look for examples of DUF3494s that come from organisms that are not obviously psychrophilic. These domains could be recombinantly expressed, checked for folding by CD, and then tested for TH and IRI. Alternatively, if the DUF3494 is secreted, the protein could be recovered from the medium for testing. The discovery of a DUF3494 protein without ice-binding activity would raise the question of its function and whether or not the ice-binding DUF3494s evolved from it, or vice versa. The discontinuous beta-solenoid is such an unusual and distinctive fold that it would be beneficial to find out where and when it originated.

Acknowledgements

PLD holds the Canada Research Chair in Protein Engineering and acknowledges financial support from the Canadian Institutes of Health Research Foundation grant 353755 and the Natural Sciences and Engineering Council of Canada discovery grant RGPIN 2016-04810. MBG thanks support by the Deutsche Forschungsgemeinschaft SPP1158 (German Research Association Special Program 1158, Grant BA 3694/2-1) and the Innovation Fund from the Alfred Wegener Institute (Project MIAA). MM thanks Marina Lotti and Stefania Brocca for the fruitful suggestions and

acknowledges support by Progetto Nazionale di Ricerche in Antartide PEA 2014–2016 and the RISE-MSCA Project 'Metable'. TDRV holds a Canadian Graduate Scholarships from the National Science and Engineering Research Council (NSERC).

Conflict of interest

The authors declare no conflict of interest.

Author contributions

The manuscript was written through contributions of all authors. All authors have given approval to the final version of the manuscript.

References

1 D'Amico S, Collins T, Marx JC, Feller G & Gerday C (2006) Psychrophilic microorganisms: challenges for life. *EMBO Rep* **7**, 385–389.
2 De Maayer P, Anderson D, Cary C & Cowan DA (2014) Some like it cold: understanding the survival strategies of psychrophiles. *EMBO Rep* **15**, 508–517.
3 Feller G (2010) Protein stability and enzyme activity at extreme biological temperatures. *J Phys: Condens Matter* **22**, 323101.
4 Mazur P (1984) Freezing of living cells: mechanisms and implications. *Am J Physiol Cell Physiol* **247**, C125–C142.
5 Steponkus PL & Lynch DV (1989) Freeze/thaw-induced destabilization of the plasma membrane and the effects of cold acclimation. *J Bioenerg Biomembr* **21**, 21–41.
6 Meryman HT (1971) Osmotic stress as a mechanism of freezing injury. *Cryobiology* **8**, 489–500.
7 Bar Dolev M, Braslavsky I & Davies PL (2016) Ice-binding proteins and their function. *Annu Rev Biochem* **85**, 515–542.
8 Duman JG (2015) Animal ice-binding (antifreeze) proteins and glycolipids: an overview with emphasis on physiological function. *J Exp Biol* **218**, 1846–1855.
9 Voets IK (2017) From ice-binding proteins to bio-inspired antifreeze materials. *Soft Matter* **13**, 4808–4823.
10 Davies PL (2014) Ice-binding proteins: a remarkable diversity of structures for stopping and starting ice growth. *Trends Biochem Sci* **39**, 548–555.
11 DeVries AL & Wohlschlag DE (1969) Freezing resistance in some Antarctic fishes. *Science (New York, NY)* **163**, 1073–1075.
12 Duman JG (2001) Antifreeze and ice nucleator proteins in terrestrial arthropods. *Annu Rev Physiol* **63**, 327–357.
13 Bredow M & Walker VK (2017) Ice-binding proteins in plants. *Front Plant Sci* **8**, 2153.
14 Hoshino T, Kiriaki M, Ohgiya S, Fujiwara M, Kondo H, Nishimiya Y, Yumoto I & Tsuda S (2003) Antifreeze proteins from snow mold fungi. *Can J Bot* **81**, 1175–1181.
15 Fletcher GL, Hew CL & Davies PL (2001) Antifreeze proteins of teleost fishes. *Annu Rev Physiol* **63**, 359–390.
16 Knight CA & Duman JG (1986) Inhibition of recrystallization of ice by insect thermal hysteresis proteins: a possible cryoprotective role. *Cryobiology* **23**, 256–262.
17 Sidebottom C, Buckley S, Pudney P, Twigg S, Jarman C, Holt C, Telford J, McArthur A, Worrall D, Hubbard R *et al.* (2000) Phytochemistry - Heat-stable antifreeze protein from grass. *Nature* **406**, 256.
18 Guo S, Garnham CP, Whitney JC, Graham LA & Davies PL (2012) Re-evaluation of a bacterial antifreeze protein as an adhesin with ice-binding activity. *PLoS ONE* **7**, e48805.
19 Guo S, Stevens CA, Vance TDR, Olijve LLC, Graham LA, Campbell RL, Yazdi SR, Escobedo C, Bar-Dolev M & Yashunsky V (2017) Structure of a 1.5-MDa adhesin that binds its Antarctic bacterium to diatoms and ice. *Sci Adv* **3**, e1701440.
20 Raymond JA, Janech MG & Fritsen CH (2009) Novel ice-binding proteins from a psychrophilic antarctic alga (Chlamydomonadaceae, Chlorophyceae) 1. *J Phycol* **45**, 130–136.
21 Bayer-Giraldi M, Weikusat I, Besir H & Dieckmann G (2011) Characterization of an antifreeze protein from the polar diatom *Fragilariopsis cylindrus* and its relevance in sea ice. *Cryobiology* **63**, 210–219.
22 Bayer-Giraldi M, Sazaki G, Nagashima K, Kipfstuhl S, Vorontsov DA & Furukawa Y (2018) Growth suppression of ice crystal basal face in the presence of a moderate ice-binding protein does not confer hyperactivity. *Proc Natl Acad Sci USA* **115**, 7479–7484.
23 Raymond JA (2011) Algal ice-binding proteins change the structure of sea ice. *Proc Natl Acad Sci USA* **108**, E198.
24 Raymond JA (2016) Dependence on epiphytic bacteria for freezing protection in an Antarctic moss, *Bryum argenteum*. *Environ Microbiol Rep* **8**, 14–19.
25 Davies PL (2016) Antarctic moss is home to many epiphytic bacteria that secrete antifreeze proteins. *Environ Microbiol Rep* **8**, 1–2.
26 Raymond JA & DeVries AL (1977) Adsorption inhibition as a mechanism of freezing resistance in polar fishes. *Proc Natl Acad Sci USA* **74**, 2589–2593.
27 Knight CA & Devries AL (1989) Melting inhibition and superheating of ice by an antifreeze glycopeptide. *Science* **245**, 505–507.

28 Celik Y, Graham LA, Mok Y-F, Bar M, Davies PL & Braslavsky I (2010) Superheating of ice crystals in antifreeze protein solutions. *Proc Natl Acad Sci USA* **107**, 5423–5428.
29 Kristiansen E & Zachariassen KE (2005) The mechanism by which fish antifreeze proteins cause thermal hysteresis. *Cryobiology* **51**, 262–280.
30 Braslavsky I & Drori R (2013) LabVIEW-operated novel nanoliter osmometer for ice binding protein investigations. *J Vis Exp* **72**, e4189.
31 Bar-Dolev M, Celik Y, Wettlaufer JS, Davies PL & Braslavsky I (2012) New insights into ice growth and melting modifications by antifreeze proteins. *J R Soc Interface* **9**, 3249–3259.
32 Scotter AJ, Marshall CB, Graham LA, Gilbert JA, Garnham CP & Davies PL (2006) The basis for hyperactivity of antifreeze proteins. *Cryobiology* **53**, 229–239.
33 Knight CA, De Vries AL & Oolman LD (1984) Fish antifreeze protein and the freezing and recrystallization of ice. *Nature* **308**, 295–296.
34 Capicciotti CJ, Doshi M & Ben RN (2013) Ice recrystallization inhibitors: from biological antifreezes to small molecules. In Recent Developments in the Study of Recrystallization (Wilson P, ed), pp. 177–224. InTech, New York, NY.
35 Knight CA, Hallett J & DeVries AL (1988) Solute effects on ice recrystallization: an assessment technique. *Cryobiology* **25**, 55–60.
36 Phippen SW, Stevens CA, Vance TDR, King NP, Baker D & Davies PL (2016) Multivalent display of antifreeze proteins by fusion to self-assembling protein cages enhances ice-binding activities. *Biochemistry* **55**, 6811–6820.
37 Budke C, Heggemann C, Koch M, Sewald N & Koop T (2009) Ice recrystallization kinetics in the presence of synthetic antifreeze glycoprotein analogues using the framework of LSW theory. *J Phys Chem B* **113**, 2865–2873.
38 Budke C, Dreyer A, Jaeger J, Gimpel K, Berkemeier T, Bonin AS, Nagel L, Plattner C, DeVries AL & Sewald N (2014) Quantitative efficacy classification of ice recrystallization inhibition agents. *Cryst Growth Des* **14**, 4285–4294.
39 Olijve LLC, Meister K, DeVries AL, Duman JG, Guo S, Bakker HJ & Voets IK (2016) Blocking rapid ice crystal growth through nonbasal plane adsorption of antifreeze proteins. *Proc Natl Acad Sci USA* **113**, 3740–3745.
40 Middleton AJ, Brown AM, Davies PL & Walker VK (2009) Identification of the ice-binding face of a plant antifreeze protein. *FEBS Lett* **583**, 815–819.
41 Smallwood M, Worrall D, Byass L, Elias L, Ashford D, Doucet CJ, Chris H, Telford J, Lillford P & Bowles DJ (1999) Isolation and characterization of a novel antifreeze protein from carrot (Daucus carota). *Biochem J* **340**, 385–391.
42 Bayer-Giraldi M, Uhlig C, John U, Mock T & Valentin K (2010) Antifreeze proteins in polar sea ice diatoms: diversity and gene expression in the genus Fragilariopsis. *Environ Microbiol* **12**, 1041–1052.
43 Takamichi M, Nishimiya Y, Miura A & Tsuda S (2007) Effect of annealing time of an ice crystal on the activity of type III antifreeze protein. *FEBS J* **274**, 6469–6476.
44 Vorontsov DA, Sazaki G, Titaeva EK, Kim EL, Bayer-Giraldi M & Furukawa Y (2018) Growth of ice crystals in the presence of type III antifreeze protein. *Cryst Growth Des* **18**, 2563–2571.
45 Garnham CP, Natarajan A, Middleton AJ, Kuiper MJ, Braslavsky I & Davies PL (2010) Compound ice-binding site of an antifreeze protein revealed by mutagenesis and fluorescent tagging. *Biochemistry* **49**, 9063–9071.
46 Garnham CP, Campbell RL & Davies PL (2011) Anchored clathrate waters bind antifreeze proteins to ice. *Proc Natl Acad Sci USA* **108**, 7363–7367.
47 Davies PL & Hew CL (1990) Biochemistry of fish antifreeze proteins. *FASEB J* **4**, 2460–2468.
48 Sicheri F & Yang DSC (1995) Ice-binding structure and mechanism of an antifreeze protein from winter flounder. *Nature* **375**, 427–431.
49 Liu Y, Li Z, Lin Q, Kosinski J, Seetharaman J, Bujnicki JM, Sivaraman J & Hew C-L (2007) Structure and evolutionary origin of Ca2+-dependent herring type II antifreeze protein. *PLoS ONE* **2**, e548.
50 Jia Z, DeLuca CI, Chao H & Davies PL (1996) Structural basis for the binding of a globular antifreeze protein to ice. *Nature* **384**, 285–288.
51 Chen LB, DeVries AL & Cheng CHC (1997) Convergent evolution of antifreeze glycoproteins in Antarctic notothenioid fish and Arctic cod. *Proc Natl Acad Sci USA* **94**, 3817–3822.
52 Graham LA, Hobbs RS, Fletcher GL & Davies PL (2013) Helical antifreeze proteins have independently evolved in fishes on four occasions. *PLoS ONE* **8**, e81285.
53 Liou Y-C, Tocilj A, Davies PL & Jia Z (2000) Mimicry of ice structure by surface hydroxyls and water of a β-helix antifreeze protein. *Nature* **406**, 322–324.
54 Hakim A, Nguyen JB, Basu K, Zhu DF, Thakral D, Davies PL, Isaacs FJ, Modis Y & Meng W (2013) Crystal structure of an insect antifreeze protein and its implications for ice binding. *J Biol Chem* **288**, 12295–12304.
55 Graether SP, Kuiper MJ, Gagne SM, Walker VK, Jia ZC, Sykes BD & Davies PL (2000) beta-helix structure and ice-binding properties of a hyperactive antifreeze protein from an insect. *Nature* **406**, 325–328.

56 Middleton AJ, Marshall CB, Faucher F, Bar-Dolev M, Braslavsky I, Campbell RL, Walker VK & Davies PL (2012) Antifreeze protein from freeze-tolerant grass has a beta-roll fold with an irregularly structured ice-binding site. *J Mol Biol* **416**, 713–724.
57 Garnham CP, Gilbert JA, Hartman CP, Campbell RL, Laybourn-Parry J & Davies PL (2008) A Ca2+-dependent bacterial antifreeze protein domain has a novel beta-helical ice-binding fold. *Biochem J* **411**, 171–180.
58 Pentelute BL, Gates ZP, Tereshko V, Dashnau JL, Vanderkooi JM, Kossiakoff AA & Kent SBH (2008) X-ray structure of snow flea antifreeze protein determined by racemic crystallization of synthetic protein enantiomers. *J Am Chem Soc* **130**, 9695–9701.
59 Lin F-H, Graham LA, Campbell RL & Davies PL (2007) Structural modeling of snow flea antifreeze protein. *Biophys J* **92**, 1717–1723.
60 Kondo H, Hanada Y, Sugimoto H, Hoshino T, Garnham CP, Davies PL & Tsuda S (2012) Ice-binding site of snow mold fungus antifreeze protein deviates from structural regularity and high conservation. *Proc Natl Acad Sci USA* **109**, 9360–9365.
61 Do H, Lee JH, Lee SG & Kim HJ (2012) Crystallization and preliminary X-ray crystallographic analysis of an ice-binding protein (FfIBP) from *Flavobacterium frigoris* PS1. *Acta Crystallogr, Sect F: Struct Biol Cryst Commun* **68**, 806–809.
62 Finn RD, Coggill P, Eberhardt RY, Eddy SR, Mistry J, Mitchell AL, Potter SC, Punta M, Qureshi M & Sangrador-Vegas A (2016) The Pfam protein families database: towards a more sustainable future. *Nucleic Acids Res* **44**, D279–D285.
63 Sorhannus U (2011) Evolution of antifreeze protein genes in the diatom genus fragilariopsis: evidence for horizontal gene transfer, gene duplication and episodic diversifying selection. *Evol Bioinform Online* **7**, 279.
64 Raymond JA & Kim HJ (2012) Possible role of horizontal gene transfer in the colonization of sea ice by algae. *PLoS ONE* **7**, e35968.
65 Raymond JA (2014) The ice-binding proteins of a snow alga, *Chloromonas brevispina*: probable acquisition by horizontal gene transfer. *Extremophiles* **18**, 987–994.
66 Uhlig C, Kilpert F, Frickenhaus S, Kegel JU, Krell A, Mock T, Valentin K & Beszteri B (2015) *In situ* expression of eukaryotic ice-binding proteins in microbial communities of Arctic and Antarctic sea ice. *ISME J* **9**, 2537–2540.
67 Goodacre NF, Gerloff DL & Uetz P (2014) Protein domains of unknown function are essential in bacteria. *MBio* **5**, e00744-13.
68 Bowman JP (2017) Genomics of Psychrophilic bacteria and Archaea. In Psychrophiles: From Biodiversity to Biotechnology (Margesin R, ed), pp. 345–387. Springer, New York, NY.
69 McBride MJ & Nakane D (2015) Flavobacterium gliding motility and the type IX secretion system. *Curr Opin Microbiol* **28**, 72–77.
70 Mangiagalli M, Bar-Dolev M, Tedesco P, Natalello A, Kaleda A, Brocca S, Pascale D, Pucciarelli S, Miceli C & Bravslavsky I (2017) Cryo-protective effect of an ice-binding protein derived from Antarctic bacteria. *FEBS J* **284**, 163–177.
71 Gwak IG, sic Jung W, Kim HJ, Kang S-H & Jin E (2010) Antifreeze protein in Antarctic marine diatom, *Chaetoceros neogracile*. *Mar Biotechnol* **12**, 630–639.
72 Vance TDR, Graham LA & Davies PL (2018) An ice-binding and tandem beta-sandwich domain-containing protein in *Shewanella frigidimarina* is a potential new type of ice adhesin. *FEBS J* **285**, 1511–1527.
73 Cheng J, Hanada Y, Miura A, Tsuda S & Kondo H (2016) Hydrophobic ice-binding sites confer hyperactivity of an antifreeze protein from a snow mold fungus. *Biochem J* **473**, 4011–4026.
74 Hanada Y, Nishimiya Y, Miura A, Tsuda S & Kondo H (2014) Hyperactive antifreeze protein from an Antarctic sea ice bacterium *Colwellia* sp has a compound ice-binding site without repetitive sequences. *FEBS J* **281**, 3576–3590.
75 Wang C, Oliver EE, Christner BC & Luo B-H (2016) Functional Analysis of a bacterial antifreeze protein indicates a cooperative effect between its two ice-binding domains. *Biochemistry* **55**, 3975–3983.
76 Hashim NHF, Sulaiman S, Bakar FDA, Illias RM, Kawahara H, Najimudin N, Mahadi NM & Murad AMA (2014) Molecular cloning, expression and characterisation of Afp4, an antifreeze protein from *Glaciozyma antarctica*. *Polar Biol* **37**, 1495–1505.
77 Xiao N, Hanada Y, Seki H, Kondo H, Tsuda S & Hoshino T (2014) Annealing condition influences thermal hysteresis of fungal type ice-binding proteins. *Cryobiology* **68**, 159–161.
78 Do H, Kim SJ, Kim HJ & Lee JH (2014) Structure-based characterization and antifreeze properties of a hyperactive ice-binding protein from the Antarctic bacterium *Flavobacterium frigoris* PS1. *Acta Crystallogr Sect D: Biol Crystallogr* **70**, 1061–1073.
79 Kondo H, Mochizuki K & Bayer-Giraldi M (2018) Multiple binding modes of a moderate ice-binding protein from a polar microalga. *Phys Chem Chem Phys* **20**, 25295–25303.
80 Lee JH, Park AK, Do H, Park KS, Moh SH, Chi YM & Kim HJ (2012) Structural basis for antifreeze activity of ice-binding protein from arctic yeast. *J Biol Chem* **287**, 11460–11468.
81 Mangiagalli M, Sarusi G, Kaleda A, Bar Dolev M, Nardone V, Vena VF, Braslavsky I, Lotti M & Nardini M (2018) Structure of a bacterial ice binding

protein with two faces of interaction with ice. *FEBS J* **285**, 1653–1666.
82 Wang C, Pakhomova S, Newcomer ME, Christner BC & Luo B-H (2017) Structural basis of antifreeze activity of a bacterial multi-domain antifreeze protein. *PLoS ONE* **12**, e0187169.
83 Leo JC, Grin I & Linke D (2012) Type V secretion: mechanism (s) of autotransport through the bacterial outer membrane. *Philos Trans R Soc Lond B Biol Sci* **367**, 1088–1101.
84 Mazmanian SK, Liu G, Ton-That H & Schneewind O (1999) Staphylococcus aureus sortase, an enzyme that anchors surface proteins to the cell wall. *Science* **285**, 760–763.
85 Janech MG, Krell A, Mock T, Kang JS & Raymond JA (2006) Ice-binding proteins from sea ice diatoms (bacillariophyceae) 1. *J Phycol* **42**, 410–416.
86 Raymond JA, Fritsen C & Shen K (2007) An ice-binding protein from an Antarctic sea ice bacterium. *FEMS Microbiol Ecol* **61**, 214–221.
87 Arai T, Fukami D, Hoshino T, Kondo H & Tsuda S (2018) Ice-binding proteins from the fungus *Antarctomyces psychrotrophicus* possibly originate from two different bacteria through horizontal gene transfer. *FEBS J* [Epub ahead of print]. https://doi.org/10.1111/febs.14725
88 Keeling PJ & Palmer JD (2008) Horizontal gene transfer in eukaryotic evolution. *Nat Rev Genet* **9**, 605–618.
89 Graham LA, Lougheed SC, Ewart KV & Davies PL (2008) Lateral transfer of a lectin-like antifreeze protein gene in fishes. *PLoS ONE* **3**, e2616.
90 Bayer-Giraldi M (2011) Antifreeze proteins from the sea ice diatom *Fragilariopsis cylindrus*. PhD thesis, Bremen University.
91 Collins RE & Deming JW (2011) Abundant dissolved genetic material in Arctic sea ice Part I: extracellular DNA. *Polar Biol* **34**, 1819–1830.
92 Lorenz MG, Aardema BW & Wackernagel W (1988) Highly efficient genetic transformation of *Bacillus subtilis* attached to sand grains. *Microbiology* **134**, 107–112.
93 Kiko R (2010) Acquisition of freeze protection in a sea-ice crustacean through horizontal gene transfer? *Polar Biol* **33**, 543–556.
94 Fitzpatrick DA (2012) Horizontal gene transfer in fungi. *FEMS Microbiol Lett* **329**, 1–8.
95 Roelofs J & Van Haastert PJM (2001) Genomics: genes lost during evolution. *Nature* **411**, 1013–1014.
96 Basu K, Garnham CP, Nishimiya Y, Tsuda S, Braslavsky I & Davies P (2014) Determining the ice-binding planes of antifreeze proteins by fluorescence-based ice plane affinity. *J Vis Exp* **83**, e51185.
97 Zepeda S, Yokoyama E, Uda Y, Katagiri C & Furukawa Y (2008) *In situ* observation of antifreeze glycoprotein kinetics at the ice interface reveals a two-step reversible adsorption mechanism. *Cryst Growth Des* **8**, 3666–3672.
98 Knight CA, Cheng CC & DeVries AL (1991) Adsorption of alpha-helical antifreeze peptides on specific ice crystal surface planes. *Biophys J* **59**, 409–418.
99 Knight CA, Wierzbicki A, Laursen RA & Zhang W (2001) Adsorption of biomolecules to ice and their effects upon ice growth. 1. Measuring adsorption orientations and initial results. *Cryst Growth Des* **1**, 429–438.
100 Kaleda A, Haleva L, Sarusi G, Pinsky T, Mangiagalli M, Bar-Dolev M, Lotti M, Nardini M & Braslavsky I (2018) Saturn-shaped ice burst pattern and fast basal binding of an ice-binding protein from an Antarctic bacterial consortium. *Langmuir* [Epub ahead of print]. https://doi.org/10.1021/acs.langmuir.8b01914
101 Graham LA, Agrawal P, Oleschuk RD & Davies PL (2018) High-capacity ice-recrystallization endpoint assay employing superhydrophobic coatings that is equivalent to the 'splat'assay. *Cryobiology* **81**, 138–144.
102 Peng Z, Peralta MDR & Toney MD (2017) Extraordinarily stable amyloid fibrils engineered from structurally defined β-solenoid proteins. *Biochemistry* **56**, 6041–6050.
103 Peralta MDR, Karsai A, Ngo A, Sierra C, Fong KT, Hayre NR, Mirzaee N, Ravikumar KM, Kluber AJ & Chen X (2015) Engineering amyloid fibrils from β-solenoid proteins for biomaterials applications. *ACS Nano* **9**, 449–463.
104 Banach M, Konieczny L & Roterman I (2018) Why do antifreeze proteins require a solenoid? *Biochimie* **144**, 74–84.
105 Bryan AW, Starner-Kreinbrink JL, Hosur R, Clark PL & Berger B (2011) Structure-based prediction reveals capping motifs that inhibit β-helix aggregation. *Proc Natl Acad Sci USA* **108**, 11099–11104.
106 Raetz CRH & Roderick SL (1995) A left-handed parallel β helix in the structure of UDP-N-acetylglucosamine acyltransferase. *Science* **270**, 997–1000.
107 Richardson JS & Richardson DC (2002) Natural β-sheet proteins use negative design to avoid edge-to-edge aggregation. *Proc Natl Acad Sci USA* **99**, 2754–2759.
108 Baardsnes J, Kuiper MJ & Davies PL (2003) Antifreeze protein dimer when two ice-binding faces are better than one. *J Biol Chem* **278**, 38942–38947.
109 DeLuca CI, Comley R & Davies PL (1998) Antifreeze proteins bind independently to ice. *Biophys J* **74**, 1502–1508.
110 Marshall CB, Daley ME, Sykes BD & Davies PL (2004) Enhancing the activity of a β-helical antifreeze protein by the engineered addition of coils. *Biochemistry* **43**, 11637–11646.

111 Kuiper MJ, Lankin C, Gauthier SY, Walker VK & Davies PL (2003) Purification of antifreeze proteins by adsorption to ice. *Biochem Biophys Res Comm* **300**, 645–648.
112 Adar C, Sirotinskaya V, Dolev MB, Friehmann T & Braslavsky I (2018) Falling water ice affinity purification of ice-binding proteins. *Sci Rep* **8**, 11046.
113 Lin F-H, Davies PL & Graham LA (2011) The Thr- and Ala-rich hyperactive antifreeze protein from inchworm folds as a flat silk-like β-helix. *Biochemistry* **50**, 4467–4478.
114 Basu K, Graham LA, Campbell RL & Davies PL (2015) Flies expand the repertoire of protein structures that bind ice. *Proc Natl Acad Sci USA* **112**, 737–742.
115 Yang J & Zhang Y (2015) I-TASSER server: new development for protein structure and function predictions. *Nucleic Acids Res* **43**, W174–W181.